Int. J. Nanosci. Nanotechnol., Vol. 9, No. 1, March 2013, pp. 7-14

Chemical Synthesis and Characterization of Perovskite $NdfeO_3$ Nanocrystals via a Co-Precipitation Method

M. Khorasani-Motlagh*, M. Noroozifar, M. Yousefi, Sh. Jahani

Department of Chemistry, Faculty of Science, University of Sistan & Baluchestan, Zahedan, I.R. Iran

(*) Corresponding author: mkhorasani@chem.usb.ac.ir
(Received:21 Dec. 2012 and Accepted: 28 March 2013)

Abstract:
A facile co-precipitation method for the synthesis of well-dispersed $NdFeO_3$ nanocrystals is developed in the presence of octanoic acid as surfactant. Co-precipitation can produce fine, high-purity, stoichiometric particles of single and multicomponent metal oxides. The product is characterized by Fourier transform infrared spectroscopy (FT-IR), X-ray diffraction (XRD), scanning electron microscopy (SEM), and energy dispersive X-ray spectrometer (EDX). The XRD analysis shows only the pattern corresponding to perovskite-type $NdFeO_3$ which crystallizes in the orthorhombic system. The spherical $NdFeO_3$ nanocrystals with an average particle size of about 69 nm can be obtained at a relatively high calcining temperature of 800°C. Also, sphere-like $NdFeO_3$ nanocrystals obtained by this method are uniform in both morphology and particle size. The results indicate that the amount of surfactant, pH and rate of stirring have an important role in the homogeneity and size of product. The preparation process can be also applied to synthesize other metal oxides.
Keywords: *Nanocrystals, Co-precipitation, Octanoic acid, Perovskite, $NdFeO_3$.*

1. INTRODUCTION

Metal particles smaller than 100 nm in primary particle diameter are generally considered as nanoparticles. Such metal nanoparticles often exhibit very interesting electronic, magnetic, optical, and chemical properties [1]. For example, their high surface-to-volume ratios have large fractions of metal atoms at surface available for catalysis [2, 3]. The vast majority of catalysts used in modern chemical industry are based on mixed metal oxides including perovskite oxides ABO_3, where A is a rare-earth element, and B is 3d transition metal remain prominent [4]. Also, perovskite oxides crystals can have broad applications in advanced technologies such as solid oxide fuel cells, catalysts and chemical sensors, magnetic materials, electrode materials, etc [5-7].

$NdFeO_3$ is known to be orthorhombically distorted perovskite structure [8]. In $NdFeO_3$ there are three major magnetic interactions: Fe–Fe, Nd–Fe and Nd–Nd [9]. These competing interactions determine their interesting structural and magnetic properties and lead to a number of applications. One application of $NdFeO_3$ nanopowders is in efficient gas sensors for H_2S [10] and C_2H_5OH [11] detection. The preparation of rare earth orthoferrites have been achieved by many methods, including hydrothermal [12], combustion [13, 14], sol-gel [15], precipitation methods [16] and sonication assisted precipitation [17].

In this paper, a simple co-precipitation procedure to prepare orthoferrite neodymium nanocrystals ($NdFeO_3$) in aqueous solution at relatively high temperature was presented. The crystalline phase with perovskite structure can be obtained by

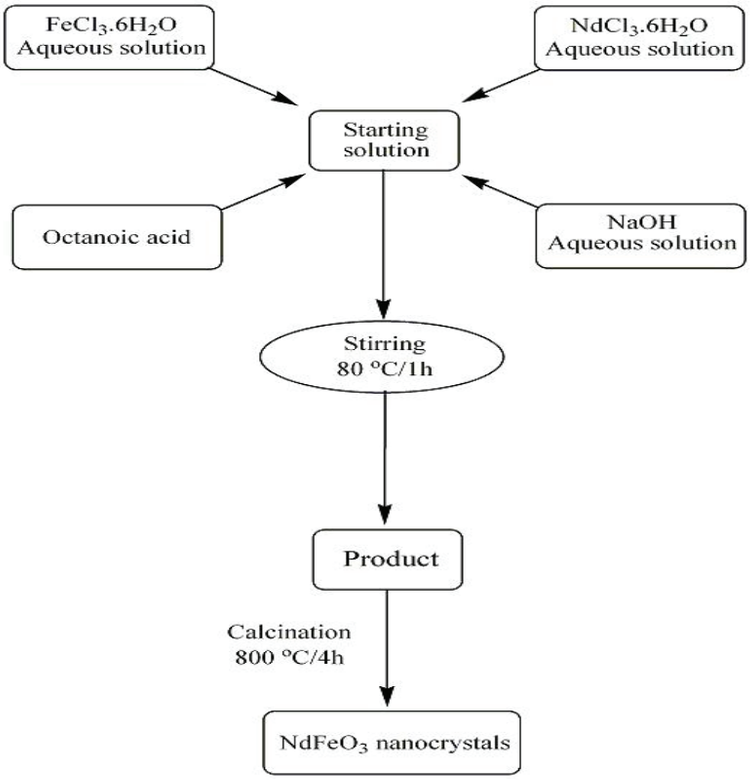

Figure 1: *Diagram of the chemical process for the formation of $NdFeO_3$ nanocrystals.*

calcining the precursor at 800°C. Co-precipitation can produce fine, high-purity, stoichiometric particles of single and multicomponent metal oxides. Furthermore, if process conditions such as solution pH, reaction temperature, stirring rate, metal salts concentration and surfactant concentration are carefully controlled, oxide particles of the desired shape and sizes can be produced.

2. EXPERIMENTAL

2.1. Material and characterization

All of the chemical reagents were of analytical grade and were used without further purification. Double distilled, deionized water was used as a solvent. Manipulations and reactions were carried out in air without the protection of nitrogen or inert gas.
Crystal structure identification was done by X-ray diffraction (XRD) using a Philips analytical PC-APD X-ray diffractometer with Cu Kα (λ = 1.54056 Å) radiation. Fourier transform infrared (FT-IR) spectra were recorded on a JASCO FT-IR 460 plus spectrophotometer using KBr pellets. Scanning electron microscopy (SEM) images were taken on a Philips XL-30ESEM equipped with an energy dispersive X-ray (EDX) spectroscopy.

2.2. Synthesis of $NdFeO_3$ nanocrystals

In a typical synthesis, a 0.1 M (10 ml) solution of iron chloride ($FeCl_3.6H_2O$) and a 0.1 M (10 ml) solution of neodymium chloride ($NdCl_3.6H_2O$) were mixed in double distilled deionized water. Deionized distilled water was used as the solvent in order to avoid the production of impurities in the final product. A specified amount of octanoic acid was added to the solution as a surfactant and coating material. A 1.5 M (25 ml) solution of sodium hydroxide (NaOH) was prepared and slowly added to the salt solution dropwise. The pH of the solution

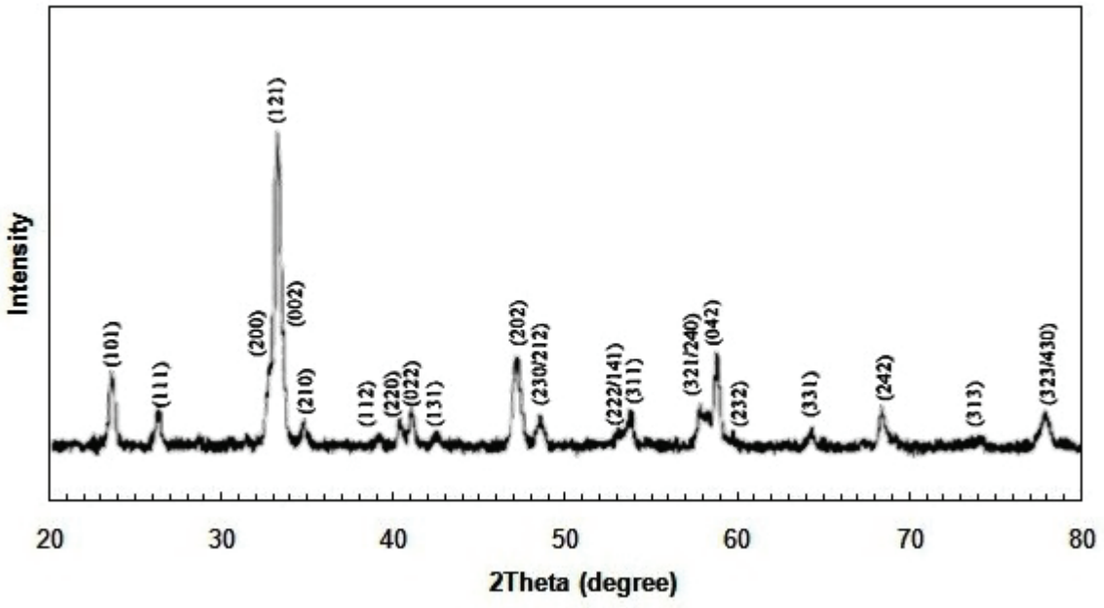

Figure 2: *XRD pattern of the $NdFeO_3$ nanocrystals.*

was constantly monitored as the NaOH solution was added. The reactants were constantly stirred using a magnetic stirrer until a pH level of 7–8 was reached. The liquid precipitate was then brought to a reaction temperature of 80˚C and stirred for 1 h. The product was then cooled to room temperature. To get particles free from sodium and chlorine compounds, the precipitate was washed twice with distilled water and then with ethanol to remove the excess surfactant from the solution. To isolate the supernatant liquid, the beaker contents were then centrifuged for 15 min at 3000 rpm. The supernatant liquid was then decanted, and then centrifuged until only thick brown precipitate remained. The obtained products were dried at 100˚C for 2 h. The acquired substance was then ground into a fine powder. At this stage the product ($NdFeO_3$) contains some associated water (up to 10 wt %), which was then removed by heating at 800˚C for 4 h (Scheme 1). The final samples were then confirmed by different techniques, such as XRD, SEM, EDX, etc.

3. RESULTS AND DISCUSSION

In Figure 2, the XRD pattern of obtained product by co-precipitation method is shown. The XRD analysis shows only the pattern corresponding to perovskite-type $NdFeO_3$ (JCPDS File no. 25-1149), which crystallizes in the orthorhombic system with a main diffraction peak at d = 2.723 Å ((1 2 1) plane). No peaks attributable to Nd_2O_3 and/or Fe_2O_3 were observed and the compound was completely decomposed to single-phase $NdFeO_3$. The sharpening of the peaks is due to the improved crystallinity of the nanoparticles and no characteristic peaks of impurities are detected in the XRD pattern. The broadening of the peaks indicates that the particles were of nanometer scale. All the characteristic peaks of $NdFeO_3$ are present and can be seen in Table 1.

The lattice parameters and cell volume were calculated by equation (1) and (2), respectively [18].

$$\frac{1}{d^2} = \frac{h^2}{a^2} + \frac{k^2}{b^2} + \frac{l^2}{c^2} \qquad (1)$$

$$V = a.b.c \qquad (2)$$

Where d is the distance between crystalline planes with Miller indices (h k l), a, b, and c are

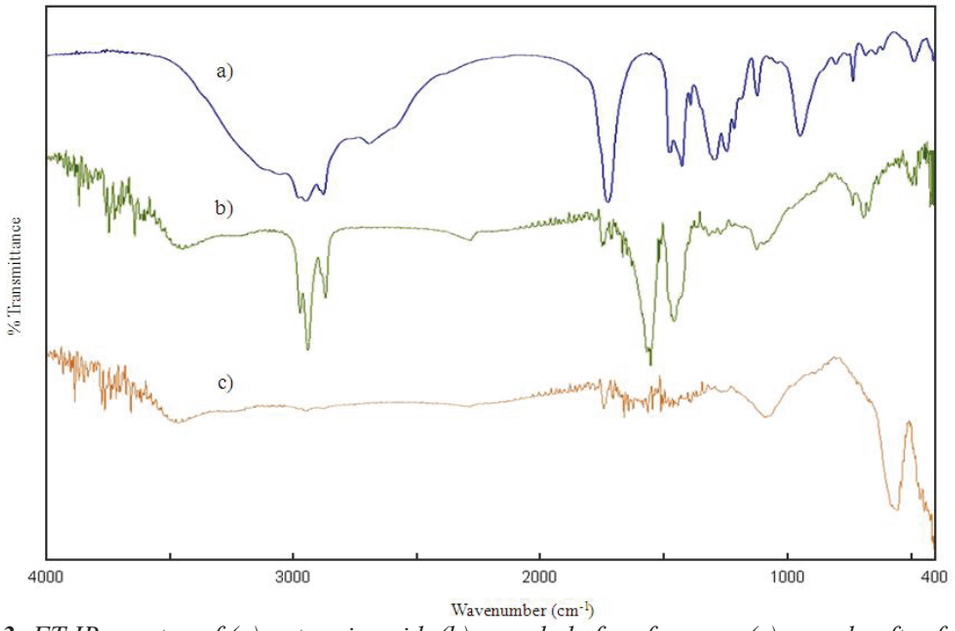

Figure 3: *FT-IR spectra of (a) octanoic acid, (b) sample before furnace, (c) sample after furnace.*

the lattice parameters, and V is cell volume. The lattice parameters and cell volume for sample were reported in Table 2, which is in good agreement with the literature values [19]. Also, the average size of the $NdFeO_3$ crystallites (D) was evaluated from XRD line broadening using the Debye-Scherrer equation [20]:

$$D = \frac{0.89\lambda}{B\cos\theta} \qquad (3)$$

where λ is the wavelength of the X-ray radiation (1.54056 Å), θ is the Bragg angle and B is the breadth of the observed diffraction line at its half maximum intensity. The average crystallite size of the $NdFeO_3$ nanoparticles is demonstrated in Table 1. FT-IR spectra of octanoic acid (a), perovskite $NdFeO_3$ before furnace (b), and perovskite $NdFeO_3$ after furnace (c), in the frequency range from 4000 to 400 cm^{-1}, are shown in Figure 3. The spectrum of the $NdFeO_3$ before furnace showed absorption band around 3000 cm^{-1} which is attributed to acid's OH that will be disappeared in spectrum after furnace. Also, the broad band in the range of 3400-3600 cm^{-1} is attributed to ν (OH) of the lattice water molecules. In the FT-IR spectrum of the final product, there are two strong absorptive bands at about 560 and 420 cm^{-1} which correspond to Fe–O stretching vibration and O–Fe–O bending vibration of perovskite $NdFeO_3$, respectively. This finding proves the formation of the perovskite $NdFeO_3$ and is in accordance with the XRD data.

The morphology, structure and particle size of the as-prepared sample were investigated by SEM. Figure 4 shows the SEM micrographs of the product. Lower magnification reveals that the product consists of loosely aggregated grains about 1 μm in size (Figure 4a). Higher magnification confirms that the grains are composed of extremely fine particles and are essentially secondary agglomerates of primary particles (Figure 4b). One can observe that nano-sized particles started to become evident within the grains and agglomerates. As it can be seen, sphere-like $NdFeO_3$ nanostructures obtained by this method are uniform in both morphology and particle size.

For further demonstration, EDX was performed on $NdFeO_3$ nanocrystals. The EDX spectrum given in Figure 5 shows the presence of neodymium and iron as the elementary components. The atomic percentage of two elements neodymium and iron is shown in Figure 5.

It is necessary to point out that the adding manner

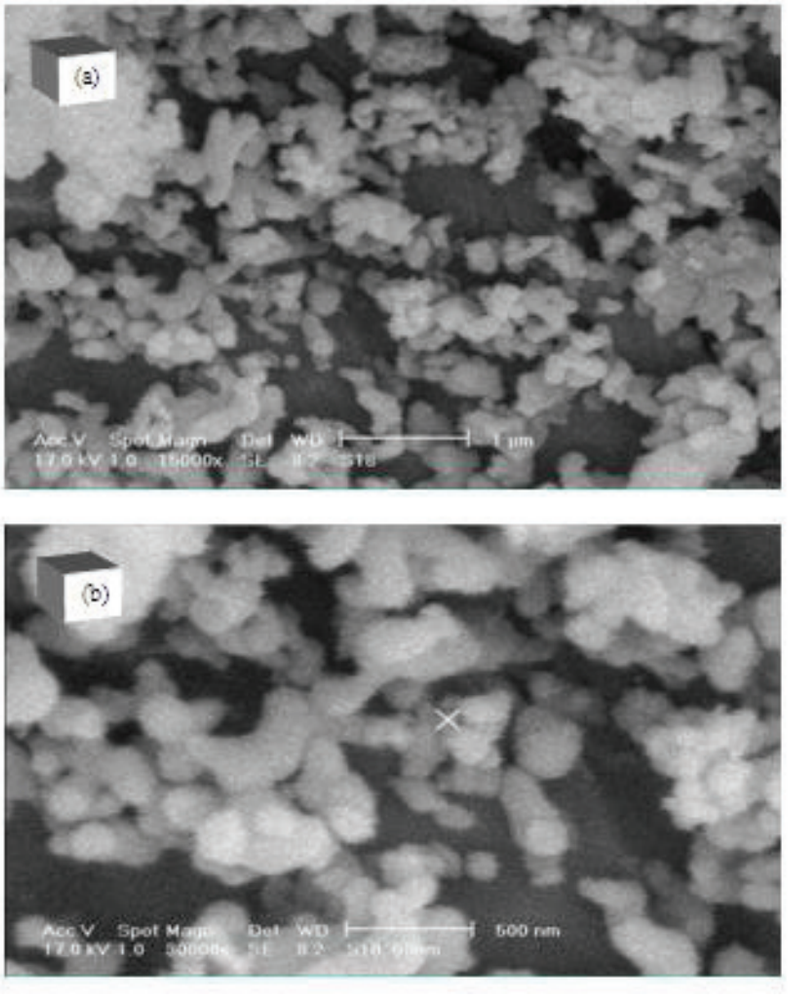

Figure 4: *SEM micrographs of $NdFeO_3$ in two different magnifications.*

of NaOH solution has an important influence on the shape of the $NdFeO_3$ nanocrystals. It is assumed that when the NaOH solution was added dropwise into the mixture solution, some small $NdFeO_3$ crystal nuclei was formed at the initial stage of the reaction. With the increase of the NaOH solution, the slowly produced $NdFeO_3$ crystallites grew along one growth direction on the basis of the initially formed $NdFeO_3$ crystal nuclei. The epitaxial growth of crystallites, the slow nucleation, and the growth rates result in the formation of nanparticles.

On the contrary, if NaOH solution was quickly added into the mixture solution, the solute was consumed rapidly and the epitaxial growth of crystallites was effectively inhibited. Meanwhile, the quick addition of NaOH solution can provide a quick rate to the crystal growth. The faster growth rate results in the crystal growth being considerably less selective in directions and hence spherical $NdFeO_3$ nanocrystals are produced.

The shape and size of $NdFeO_3$ nanocrystals can be further tuned by adding small amounts of surfactants. The result demonstrates that the presence of small amounts of octanoic acid leads to the shape change of $NdFeO_3$ products. Also, the presence of octanoic acid led the particles to be well dispersed with no agglomeration, while much larger particles

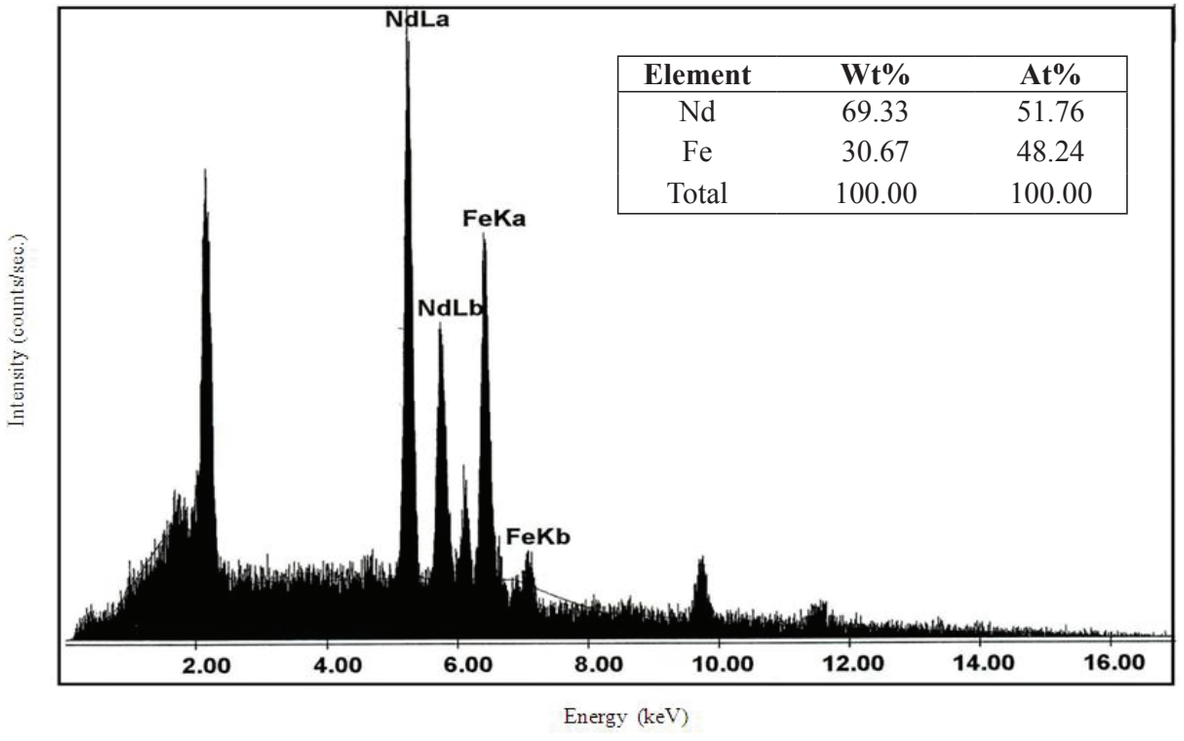

Figure 5: *EDX analysis of $NdFeO_3$ nano-sized powders.*

Table 1: *The average particle size of $NdFeO_3$ nanocrystals using of XRD pattern*

Angle [°2θ]	(h k l)	d-value α_1 [Å]	T.width [°2θ]	Size of particle [nm]	Average size [nm]
23.06	(101)	3.85	0.04	200.71	
25.94	(111)	3.43	0.28	28.82	
32.37	(200)	2.76	0.16	51.17	
32.86	(121)	2.72	0.20	40.98	
34.45	(210)	2.60	0.08	102.88	
39.99	(220)	2.25	0.10	83.62	67
40.73	(022)	2.21	0.28	29.96	
46.92	(202)	1.93	0.14	61.22	
48.32	(230/212)	1.88	0.20	43.04	
53.63	(311)	1.70	0.24	36.71	
57.72	(321/240)	1.59	0.16	56.08	
58.76	(042)	1.57	0.28	32.23	
68.45	(242)	1.37	0.24	39.60	
78.12	(323/430)	1.22	0.08	126.61	

Table 2: *Lattice parameters and size of nano perovskite–type oxide $NdFeO_3$ synthesized using co-precipitation method.*

lattice parameters (Å)			cell volume	average size (nm)	
a	b	c	V (Å³)	XRD	SEM
5.53	7.70	5.38	229.08	67	58

flocculating together were synthesized in the absent of octanoic acid. The use of a surfactant to control the morphological evolution of nanocrystals has been extensively explored. It is generally accepted that the surfactant kinetically controls the growth rates of various faces of nanocrystals by selective adsorption and desorption on these surfaces [21]. The octanoic acid may adsorb into the fastest growth face of $NdFeO_3$ nanocrystals. Hence, the epitaxial growth of nanocrystals is effectively inhibited and spherical $NdFeO_3$ nanocrystals are produced.

4. CONCLUSIONS

In summary, pure phase $NdFeO_3$ nanoparticle powder with an orthorhombic structure was synthesized successfully by co-precipitation method in the presence of octanoic acid as surfactant. The pure perovskite $NdFeO_3$ products were formed by heat treatment at 800˚C for 4 h. Co-precipitation is a suitable method for the control of nanoparticle sizes with variation of the reaction conditions. Morphology of the neodymium orthoferrite nanoparticle ($NdFeO_3$) was sphere-like nanoparticles in this method. The size of the nanocrystals was measured both by XRD and SEM and the results were in very good agreement with each other.

ACKNOWLEDGMENT

The authors are grateful to the University of Sistan and Baluchestan (USB) for providing financial support to undertake this work.

REFERENCES

1. M. Salavati-Niasari, F. Davar, M. Mazaheri, and M. Shaterian, J. Magn. Magn. Mater., Vol. 320, No. 3-4, (2008), pp. 575-578.
2. R. W. Siegel, Annu. Rev. Mater. Sci., Vol. 21, No. 1, (1991), pp. 559-578.
3. R. W. Siegel, Nanophase Materials: Synthesis, Structure, and Properties, Springer Series in Material Science, (1994); pp. 65.
4. M. A. Pena and J. L. G. Fierro, Chem. Rev., Vol. 101, No. 7, (2001), pp. 1981-2018.
5. J. F. Berry, X. Ren, J. Ramon Gancedo and F. J. Marco, Hyperfine Interact., Vol. 156-157, No. 1-4, (2004), pp. 335-340.
6. Q. Zhang, and F. Saito, J. Mater. Sci., Vol. 36, No. 9, (2001), pp. 2287-2290.
7. S. Nakayama, J. Mater. Sci., Vol. 36, No. 23, (2001), pp. 5643-5648.
8. R. Przenioslo, I. Sosnowska, M. Loewenhaupt and A.Taylor, J. Magn. Magn. Mater., Vols. 140-144, part 3, (1995), pp. 2151-2152.
9. A. Bashir, M. Ikram, R. Kumar, P. Thakur, K. H. Chae, W. K. Choi and V. R. Reddy, J. Phys.: Condens. Matter, Vol. 21, No. 32, (2009), pp. 325501.
10. N. Xinshu, D. Weimin, D. Weiping and J. Kai, J. Rare Earths, Vol. 21, No. 6, (2003), pp. 630-632.
11. X. Lou, X. Jia and J. Xu, J. Rare Earths, Vol. 23, No. 3, (2005), pp. 328-331.
12. W. Zheng, R. Liu, D. Peng and G. Meng, Mater. Lett., Vol. 43, No.1-2, (2000), pp. 19-22.

13. S. S. Manoharam and K. C. Patil, J. Solid State Chem., Vol. 102, No. 1, (1993), pp. 267-276.

14. A. Chakraborty, P. S. Devi and H. S. Maiti, J. Mater. Res., Vol. 10, No. 4, (1995), pp. 918-925.

15. H. Cui, M. Zayat and D. Levy, J. Non-Cryst. Solids, Vol. 352, No. 28-29, (2006), pp. 3035-3040.

16. H. N. Pandya, R. G. Kulkarni and P. H. Parsania, Mater. Res. Bull., Vol. 25, No. 8, (1990), pp. 1073-1077.

17. S. Singh, A. Singh, B. C. Yadav and P. K. Dwivedi, Sens. Actuators B: Chem., Vol. 177, (2013), pp. 730-739.

18. X. Ge, Y. Liu and X. Liu, Sens. Actuators B: Chem., Vol. 79, No. 2-3, (2001), pp. 171-174.

19. V. A. Streltsov and N. Ishizawa, Acta Crystallogr. B, Vol. 55, No. 1, (1999), pp. 1-7.

20. H. P. Klug and L. E. Alexander, X-ray Diffraction Procedures for Polycrystalline and Amorphous Material, second ed., Wiley, New York, (1974).

21. Y. Sun and Y. Xia, Adv. Mater., Vol. 14, No. 11, (2002), pp. 833-837.